Elastic Body Contact Simulation for Predicting Piston Slap Induced Noise in IC Engines

Günter Offner*, Hans H. Priebsch* , **

* Christian-Doppler Laboratory for Engine and Vehicle Acoustics at
Institute for Combustion Engines and Thermodynamics,
TU Graz, Austria
** AVL List GmbH, Graz, Austria

Abstract:

Piston slap induced noise may contribute significantly to the noise emitted from Internal Combustion engines in a specific frequency range. There is a high interest to simulate this phenomenon in the development process of both, Diesel and gasoline engines in order to analyse measures for reducing this noise source in an early development stage of the engine. Piston slap is mainly affected by various design parameters of piston and liner, by the temperature distribution and by the combustion timing.

The paper summarises a methodology for predicting the piston to liner contact in running engines by means of MBD (Multi-Body Dynamics) and FEM. The advantages of this methodology are precise contact modelling on one hand and freedom in the model application on the other. Thus, trends caused by changes in the piston design and of combustion parameters on the contact impact can be analysed by simulation. Contact statistics e.g. peak contact pressures and their locations, etc. help to assess the importance of the contact events.

In addition to the mathematical modelling of the excitation the paper describes the transfer mechanisms of the piston slap phenomenon. Thus, the model is extended in order to analyse vibration transfer via engine structure. Results of simulation work show structure surface velocity levels and their contribution to integral levels in different frequency bands.

2. Introduction:

For the development of all types of IC engines, the optimisation of piston to liner contact is of central importance. Its design affects key functions such as durability, performance and noise of the engine.

PDF-XCHANGE Click to buy NOW! www.docu-track.com

Designing optimum piston / liner assemblies by means of simulation can significantly reduce development cost for prototype testing work.

Besides the primary oscillating motion, the piston performs a secondary motion due to the gap between piston and cylinder liner (briefly liner). This piston secondary or slap motion (piston slap) consists of translational and rotational components. It is caused by the reaction force and torque of the con-rod small end, which may change their direction and value during the engine cycle and allow the piston to move within the existing clearance. The amount of clearance is affected by the geometry and by the elasticity of the parts in the sliding contact.

Piston to liner contact occurs directly between piston skirt and liner and indirectly via piston rings. in the running engine, the structure in the contact area is excited radially in piston slap direction, and tangentially in sliding direction. The clearance between piston skirt and liner is formed by their shapes. Each shape is caused by the manufacturing (profile) and actual deformations due to loads (e.g. temperature, gas, assembly loads). The clearance is partly filled with oil. The amount of oil filling is depending on the oil itself, on the contacting parts (piston, rings and liner) and the engine running conditions.

The piston slap motion is affecting both the contact between the sliding parts and the excitation of the structure vibration. Thus on one hand, sliding contact between piston skirt and liner directly affects wear and mechanical friction losses of the engine. Furthermore in interaction with the piston rings, effects on blow-by and LOC (lube oil consumption) can be observed.

On the other hand, piston slap is an impact phenomenon causing engine noise and cavitation of the liner in the cooling water jacket. Piston slap induced noise is known as a very significant source of noise excitation mainly existing in the 2 kHz octave band. Its reduction is more often related to customer annoyance and subjective complaints than to meet legislation limits. Well known as a possible problem for Diesel engines, it can be observed for modern Gasoline engines, too. Due to all the important influences on engine design, piston slap phenomena have been analysed by simulation [4,7] and experimental methods [2,5,8].

Using a FEM model for the entire engine and applying the relevant forces for noise excitation (gas forces, mass forces of moving crank train and valve train part, etc.) the effect of piston slap excitation can be analysed in principle. The example in figure 1 shows the calculated surface velocity levels on an envelop mesh of a 4 cylinder Diesel engine. The results show the difference of the velocities with and w/o considering precalculated excitation forces on the cylinder liners. The liner forces were simulated by a single mass moving in the actual clearance between piston and liner due to engine operating condition at 4000 rpm, full load.

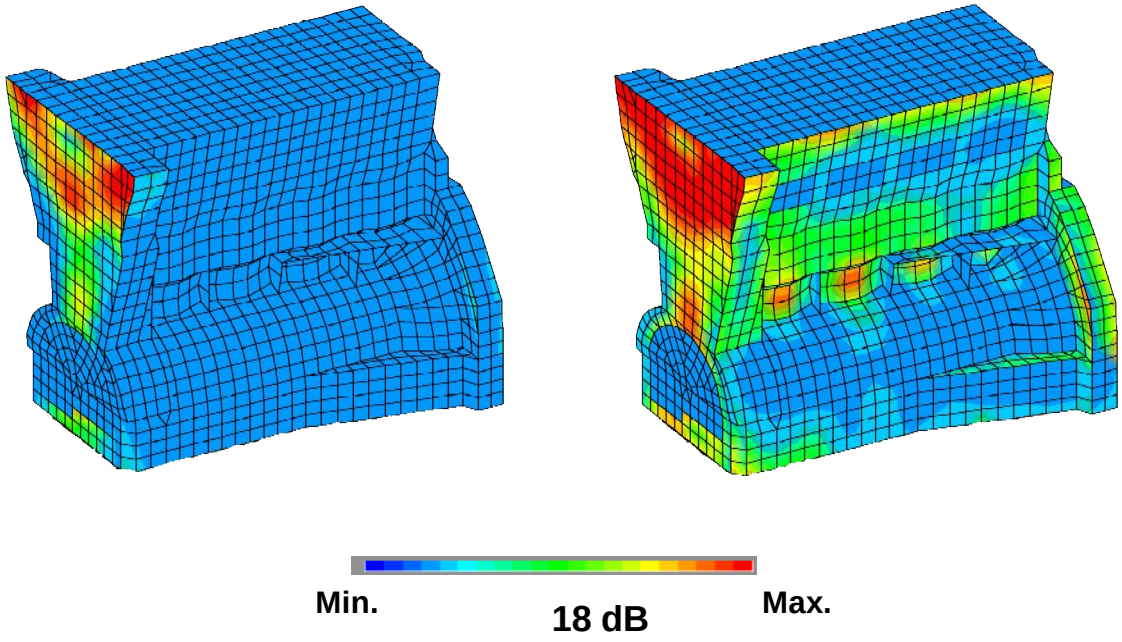

Figure 1: *Integral surface velocity level (2 kHz Octave band) of a 4 Cyl. Diesel engine w/o (left) and with (right) considering liner excitation forces.*

The spots on the right engine model in the frequency range 1400 – 2800 Hz indicate clearly the importance liner excitation for the structure borne noise. Despite showing the contributions of piston slap induced noise in principle, a model as described in figure 1 is not sufficient to analyse the effects of the piston impact events and their interaction with structure vibration as detailed as required for a noise optimisation.

For a very detailed analyses of all important parameters concerned, a simulation model has been developed by the authors based on the theory of elastic multi-body-dynamics and is described within this paper. For this first model, the assumption is made, that the contribution of piston rings to liner noise excitation is neglectable. For this reason, piston rings are considered in the calculation model by masses only. In the piston skirt contact the assumption is made, that radial excitation is dominating compared to sliding excitation. The effect of sliding excitation will be shown in a future publication. The resulting model of this paper enables analysis of design modifications, e.g. change of manufacturing profiles, piston design and offset, and to analyse their effects on the contact area.

3. Basic equations:

In this chapter the formulation of representative equations describing the mathematical simulation model and the introduction of ingenious simplifications is described. Because of the complex structure of a multi-body-system, it has to be broken down into coupled systems, consisting of bodies, e.g. piston and liner, with linear elastic behaviour and connections, e.g. lubricated regions, considering the non-linear forces, acting between the connected bodies. The basic

equations, used in case of simulation procedure of elastic piston liner contact are

- Equation of motion to compute global motions and vibrations of bodies
- Non-linear joint equations (e.g. Reynolds equation, spring-damper functions) to compute forces and moments, acting between connected bodies

2.1. Equation of motion

For calculation of motions each body has to be divided into a sufficiently high number of sub-bodies (partial masses). The dynamic behaviour of each of these rigid partial masses is given by the classical equation of motion for linear systems

$$\boldsymbol{M}\cdot\ddot{\boldsymbol{q}}+\boldsymbol{D}\cdot\dot{\boldsymbol{q}}+\boldsymbol{K}\cdot\boldsymbol{q}=\boldsymbol{f} \quad (1)$$

derived from the equations of momentum and angular momentum. $\boldsymbol{q}=[\boldsymbol{q}_1,\boldsymbol{q}_2,...,\boldsymbol{q}_n]^t$ is the generalized displacement vector for n partial masses. Each element of the vector is a vector itself with three translatorial motion components and three rotational motion components ($\boldsymbol{q}_i=[u_1,u_2,u_3,\gamma_1,\gamma_2,\gamma_3]_i^t$). Damping matrices ($\boldsymbol{D}$) are calculated from given mass matrices ($\boldsymbol{M}$) and stiffness matrices ($\boldsymbol{K}$) according to the linear combination $\boldsymbol{D}=\alpha\cdot\boldsymbol{K}+\beta\cdot\boldsymbol{M}$, in the course of which α and β are functions of the structural damping and modal frequencies. The right hand side of the equation is given by adding up the external loads ($\boldsymbol{f}^{(a)}$), exciting joint forces and moments ($\boldsymbol{f}^*$) and inertia terms ($\boldsymbol{p}^*$):

$$\boldsymbol{f}=\boldsymbol{f}^{(a)}+\boldsymbol{f}^*+\boldsymbol{p}^* \quad (2).$$

External forces (e.g. gas force) and moments are determined functions given in time, calculated from given measurement data. The non-linear terms of excitational loads are given by joints, connecting one body to another (e.g. contact forces acting between piston and liner resulting from solution of Reynolds equation). In case of bodies with global motions (e.g. piston), non-linear inertia terms, detaily discussed in [9,10], also have to be considered in the equation.

2.2. Reynolds equation

Pressure distribution of the oilfilm in a lubrication region between two elastic bodies can be calculated using Reynolds equation derived from Navier-Stokes' equation and equation of continuity:

$$-\frac{\partial}{\partial x}\left(\frac{1}{12\eta}\cdot\theta\cdot h^3\cdot\frac{\partial p}{\partial x}\right)-\frac{\partial}{\partial z}\left(\frac{1}{12\eta}\cdot\theta\cdot h^3\cdot\frac{\partial p}{\partial z}\right)+\frac{w_{Liner}+w_{Piston}}{2}\frac{\partial(h\cdot\theta)}{\partial z}+\frac{\partial(h\cdot\theta)}{\partial t}=0\,. \quad (3)$$

The derivation takes as well laminar conditions, Newton fluid properties as special geometrical assumptions (pressure is constant in direction of gap height) of the lubrication region between piston and liner into account. The shear velocity part of the equation considers the axial velocity components of both connected bodies according to the stick condition:

$$\begin{aligned} w(x,0,z,t) &= w_{Piston} \\ w(x,h,z,t) &= w_{Liner} \end{aligned} \quad . \quad (4)$$

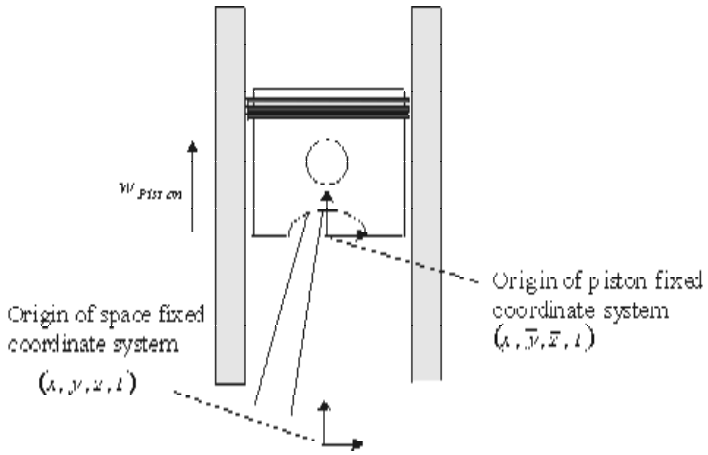

Figure 2: *Coordinate transfomation to the piston fixed coordinate system*

In order to get a time invariant calculation region, a coordinate transformation has to be done from the space fixed coordinate system (x,y,z,t) to the piston fixed coordinates $(x,\bar{y},\bar{z},t)$, where the coordinate in gap direction (y) has to be normalized (Fig. 2):

$$\begin{aligned} z &= \int_0^t w_{Piston}(\xi)d\xi + \bar{z} =: z_0(t) + \bar{z} \\ y &= \bar{y} \cdot \bar{h}(x,\bar{z},t) \end{aligned} \quad . \quad (5)$$

So, for each function f

$$\begin{aligned} f &: R^4 \ \mathbf{a}\ R \\ (x,y,z,t) &\ \mathbf{a}\ f(x,y,z,t) \end{aligned} \quad (6)$$

the corresponding function in the piston fixed coordinate system $\bar{f}$

$$\begin{array}{l} \bar{f} : R^4 \;\; \mathbf{a} \;\; R \\ (x, \bar{y}, \bar{z}, t) \;\; \mathbf{a} \;\; \bar{f}(x, \bar{y}, \bar{z}, t) \end{array} \quad (7)$$

is defined according to

$$\bar{f}(x, \bar{y}, \bar{z}, t) := f\left(x, \bar{y} \cdot \bar{h}, z_0 + \bar{z}, t\right). \quad (8)$$

Carrying out the transformation (8) for equation (3) yields to the Reynolds equation given in a piston fixed coordinate system:

$$-\frac{\partial}{\partial x}\left(\frac{1}{12\bar{\eta}} \cdot \bar{\theta} \cdot \bar{h}^3 \cdot \frac{\partial \bar{p}}{\partial x}\right) - \frac{\partial}{\partial \bar{z}}\left(\frac{1}{12\bar{\eta}} \cdot \bar{\theta} \cdot \bar{h}^3 \cdot \frac{\partial \bar{p}}{\partial \bar{z}}\right) + \frac{w_{Liner} - w_{Piston}}{2} \frac{\partial\left(\bar{h} \cdot \bar{\theta}\right)}{\partial \bar{z}} + \frac{\partial\left(\bar{h} \cdot \bar{\theta}\right)}{\partial t} = 0 \,. \quad (9)$$

Due to piston functionality and manufacturing profile, no hydrodynamic contact between piston and liner will occure in piston pin area. For that reason, the hydrodynamic calculation can be reduced to the lubricated area L in direction of TS-ATS with the bounary B. Because of the limited oil supply in the contact area L and since piston skirt and liner have not exact cylindric contours (e.g. manufacturing profile of a piston skirt, deformation due to assembly and thermal load of a liner contact surface), L can be divided into an area with hydrodynamic contact (L_C) and an area with out hydrodynamic contact ($L_{\bar{C}}$) at each discrete point of time:

$$L = L_C \cup L_{\bar{C}} \,. \quad (10)$$

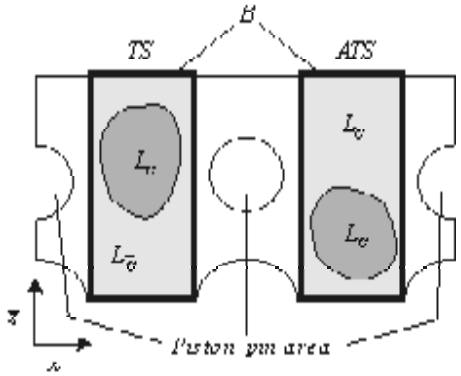

Figure 3: *Calculation regions on unrolled piston skirt surface*

4. Simulation procedure:

The simulation procedure consists of three main steps:

PDF-XCHANGE Click to buy NOW! www.docu-track.com

- Preprocessing, including generation of geometries and structural matrices for each elastic body of the multi-body model using FEM, condensation, determination of external loads and generation of contact surface profile data from real messured data for connected bodies
- Multi-body dynamics (MBD) vibration analysis in time domain, considering condensed structure matrices, non-linearities occuring at connections between the elastic bodies and loads
- Postprocessing including datarecovery to the uncondensed system and contact statistics

Stiffness and mass properties as well as geometry information can be generated using a usual FE-software package (For results shown in this paper MSC-Nastran was used.). In order to enable an efficient solution of vibration equations, a reduction (condensation) of the number of degrees of freedom has to be done. The reduced set $\boldsymbol{q}_a$ includes as well static as modal degrees of freedom and can be computed via equation (11), where $\boldsymbol{G}_{ft}$ represents the transformation matrix [1, 3]:

$$\boldsymbol{q} = \boldsymbol{G}_{ft} \cdot \boldsymbol{q}_a \,. \quad (11)$$

By this, the number of degrees of freedom can be reduced significantly (e.g. for the piston shown in figure 5 from 25000 to 700). Substitution of (11) in the equation of motion (1) and multiplication with $\boldsymbol{G}_{ft}^{t}$ from left hand side results in

$$\overline{\boldsymbol{M}} \cdot \ddot{\boldsymbol{q}}_a + \overline{\boldsymbol{D}} \cdot \dot{\boldsymbol{q}}_a + \overline{\boldsymbol{K}} \cdot \boldsymbol{q}_a = \bar{\boldsymbol{f}} \,, \quad (12)$$

where $\overline{\boldsymbol{M}}$, $\overline{\boldsymbol{D}}$ and $\overline{\boldsymbol{K}}$ denote the condensed mass, damping and stiffness matrices and $\bar{\boldsymbol{f}}$ is the condensed force vector. The reduced matrices together with the table of degrees of freedom and the node positions are taken from FE software via an interface. Vibration analysis is performed on the reduced system only.

3.1. Time integration

The condensed equation of motion, (12), for each connected body of the multi-body system together with the equations, computing the forces and moments acting between the connected bodies (e.g. Reynolds equation) yield to a total system of high complexity. Due to the non-linear characteristic of this system, it has to be solved in the time domain. In order to minimize numerical error a direct implicit integration method (Newmarks method) considering adjusted time step size is used for time integration. In each time step both the equilibrium in the equation of motion and in Reynolds equation and the equilibrium of the total system have to be fulfilled. The total system considers the interaction of excitation loads, resulting from integration of pressure distribution $\bar{p}(x,\bar{z})$, and the function of clearance height in the lubricated region between two connected bodies $\bar{h}(x,\bar{z})$:

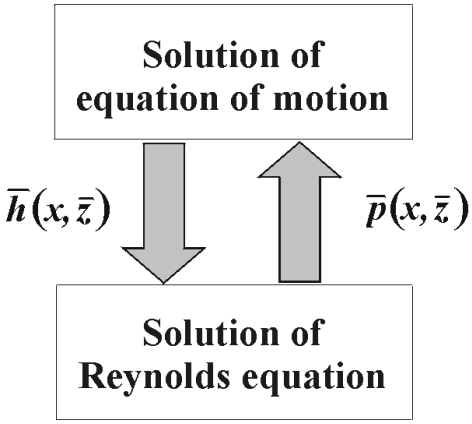

Figure 4: *Solution structure of the total system*

3.2. Solution of equation of motion

Equation (12) has to be solved in $\boldsymbol{q}_a$ with known external forces, the calculated excitation forces and moments and non-linear inertia terms. For calculation of the positions of the partial masses of a body, the equation of this body will be integrated. For the derivatives with respect to time of the vector $\boldsymbol{q}_a$, a direct implicit integration method is used ([1], [3]):

$$\begin{aligned} \dot{\boldsymbol{q}}_a &= a \cdot \boldsymbol{q}_a + \boldsymbol{b}_{q_a} \\ \ddot{\boldsymbol{q}}_a &= c \cdot \boldsymbol{q}_a + \boldsymbol{d}_{q_a} \end{aligned} \quad . \quad (13)$$

The scalar parameters a and c depend on the actual time step size and $\boldsymbol{b}_{q_a}$ and $\boldsymbol{d}_{q_a}$ are functions depending on solutions of $\boldsymbol{q}_a$, $\dot{\boldsymbol{q}}_a$ and $\ddot{\boldsymbol{q}}_a$ of former timesteps. Substitution of (13) and transformation of the resulting equation lead to a linear system for determination of the generalized displacements with the effective stiffness matrix $\hat{\boldsymbol{K}}$ and the effective load vector $\hat{\boldsymbol{f}}$:

$$\hat{\boldsymbol{K}} \cdot \boldsymbol{q}_a = \hat{\boldsymbol{f}} \quad . \quad (14)$$

Solution of this linear system can be done easily by factorization using the method of Cholesky [1].

3.3. Solution of Reynolds equation

The excitation forces needed for solving the equation of motion are calculated by integrating the oil film pressure in the clearance between the two connected bodies. The pressure distribution in the lubrication region L_C ($\theta = 1$) is calculated by solving the Reynolds

equation in the piston fixed coordinate system. The oil viscosity may be constant or it may depend on the oil film pressure obeying an exponential law:

$$\overline{\eta} = \eta_0 \cdot e^{\alpha p} \quad . \quad (15)$$

The calculation is performed on an equidistant calculation grid, moved with the piston skirt surface. Because of the regular structure of the grid nodes, a finite volume method is used for calculation. In order to get the terms resulting from the shear part of the equation, a combination of backward difference methods of second order and central difference methods of second order have to be used.

Both pressure distribution in the lubricated contact region L_C and the contact region itself, are determined iteratively. The classical SOR method (successive over relaxation) is used because of the optimal starting values for the first step of iteration that can be taken from the last time step. The relaxation parameter ω is controled considering the stability of the calculated pressure values. The usage of this relaxation method also allows the consideration of a simple cavitation algorithm: each negative pressure value is set equal to a given cavitation pressure value, that is constant [6].

4. Result Examples and Trend Analysis:

For parametrical studies, a one cylinder 4-stroke engine with 83.0 mm stroke and speed of 3000 rev/min was simulated. Both piston skirt and liner surface data were generated by a linked profile generator. In all result examples one and a half cycles were calculated. Because of simulation beginning oscillations, the first half cycle was cut off in the shown results.

The basic Finite Element models of the piston and liner structures are shown in figure 5 and figure 6. These models are generated with a constant nominal diameter of 76.0 mm. For consideration of surface profiles, surface profile data for the piston and the liner and constant values for nominal clearance were included separately. The length of liner, of piston and of piston skirt were 180 mm, 80 mm and 54.5 mm respectively. The piston pin is placed 30.5 mm from the lower edge of the skirt with no offset. The piston pin and the connecting rod are beam-mass models. The crankshaft is modelled with one node moving along a circle with constant velocity. The piston and the piston pin as well as the pin and the connecting rod, as the connecting rod and the crankshaft node, were connected via non-linear spring-damper functions.

PDF-XCHANGE
Click to buy NOW!
www.docu-track.com

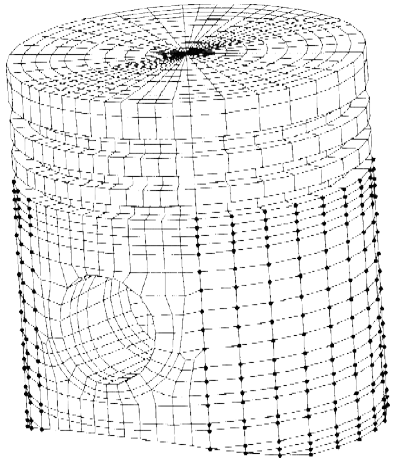

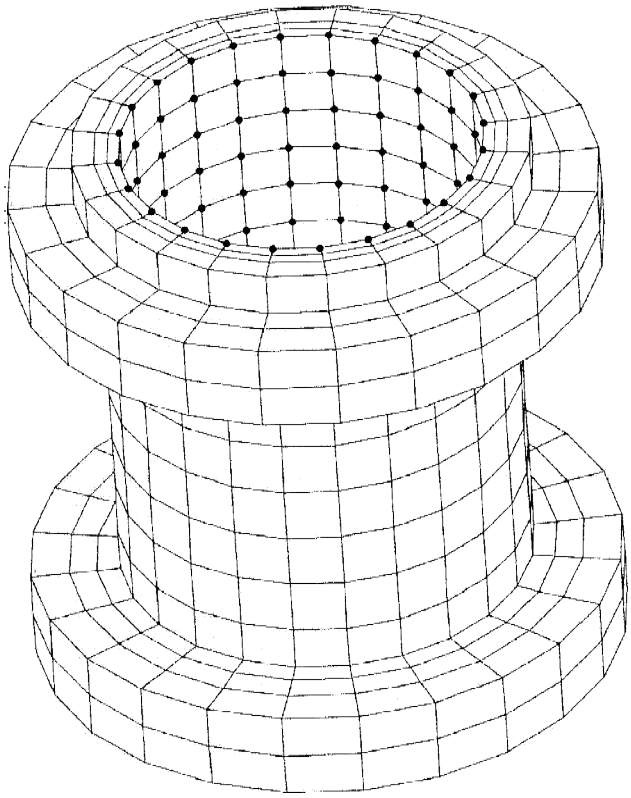

Figure 5: *FE-model of piston*
Figure 6: *FE-model of liner*

Boundary conditions for hydrodynamic calculations were set to ambient pressure at the lower and at the top edge of the piston skirt. For all calculations a constant value of $\overline{\eta} = 1.0 \cdot 10^{-8}$ Ns/mm² was used for viscosity and a constant oil height at the liner wall was predefined. Nodes, that were considered in the solution of Reynolds equation are marked with fat dots (Fig. 5, Fig. 6). Figure 7 shows the used gas force for one engine cycle that is applied to each of eight nodes at top piston surface in piston stroke direction separately.

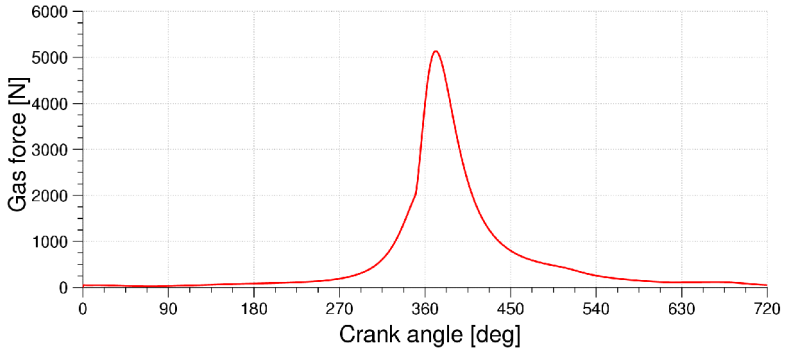

Figure 7: *Gas force*

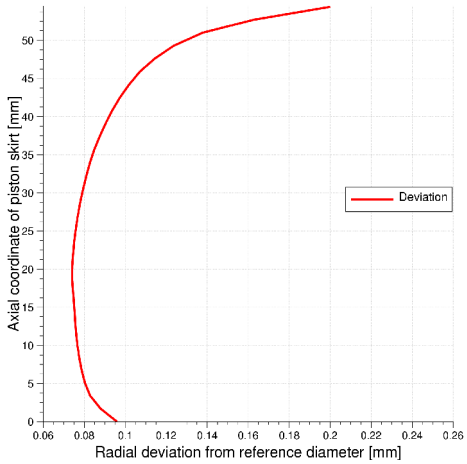

Figure 8a: *Meridian of an axial symmetrical profile of a piston skirt*

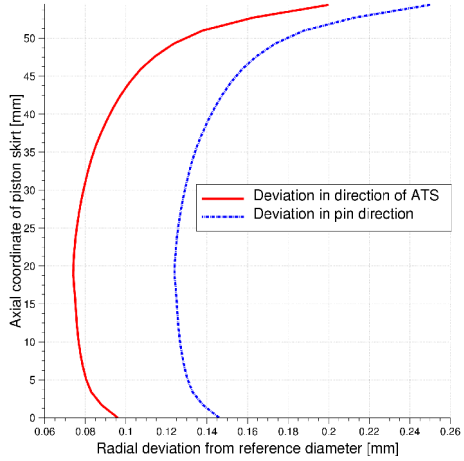

Figure 8b: *Meridians of a piston skirt profile with single ovality*

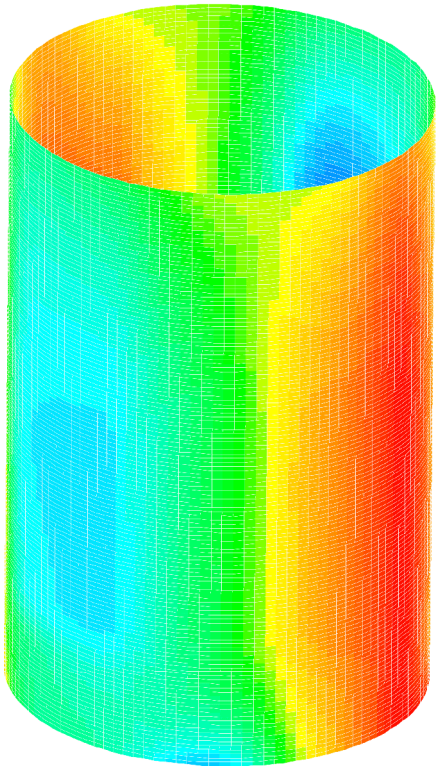

Figure 9: *Liner surface profile*

Two different types of piston profiles were tested in simulation. On one hand an axially symmetrical profile was used with maximum deviation of 0.2 mm at the upper edge of the skirt (Fig. 8a) , on the other hand a profile with single ovality considering a maximum deviation of 0.2 mm in the direction of the anti-thrust side (ATS) and a deviation of 0.25 mm in piston pin direction (Fig. 8b) was tested. The used liner surface profile (deviation from nominal diameter), calculated from measurement data, is shown in figure 9.

In order to characterize the friction loss and wear behaviour, the distribution of oilfilm thickness between two contacting bodies is of great importance. Besides the surface profile of the two bodies, the distribution is mainly influenced by the nominal radial clearance between the two bodies. The first study tries to figure out the

influence of the nominal radial clearance between piston skirt and liner. The simulation was perfomed, using two different values of nominal clearance (10 μm, 100μm) in addition with a piston surface profile with single ovality (Fig. 8b) and a constant oil heigth of 30μm at inner liner wall.

Figure 10 shows the minimal gaps between the piston skirt and cylinder liner, which value is identical with the minimum oilfilm thickness below 30μm. Differences of the two results are mainly caused by inertia effects resulting from corresponding terms in the equation of motion (1).

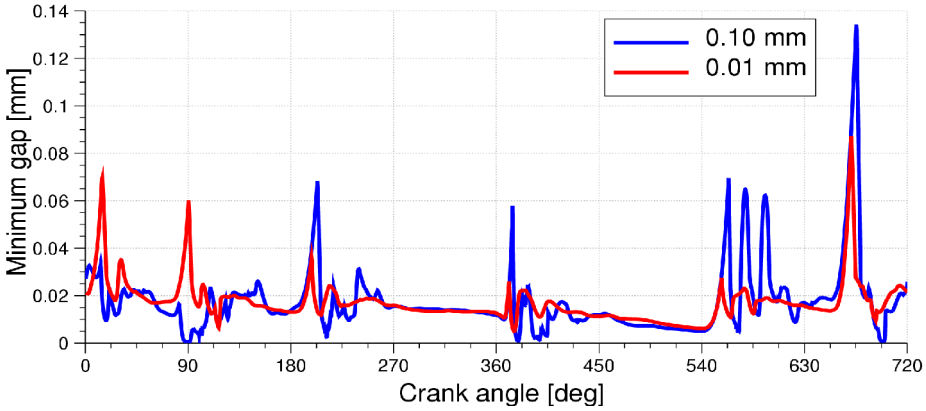

Figure 10: *Minimum gap for different nominal clearance*

In order to reveal the effect of the available oil quantity, figure 11 shows the effect of different values for available oil height at the liner wall on peak oil film pressure. Values of 30μm and 130μm were used in addition with a piston surface profile with singular ovality (Fig. 8b). The shown results underline the sensibility of the system due to oil supply. In correspondence with figure 7 the maximum oilfilm pressure values were calculated at FTDC – 7.87 MPa in the case of 130μm and 46.72 MPa in the case of 30μm.

PDF-XCHANGE
Click to buy NOW!
www.docu-track.com

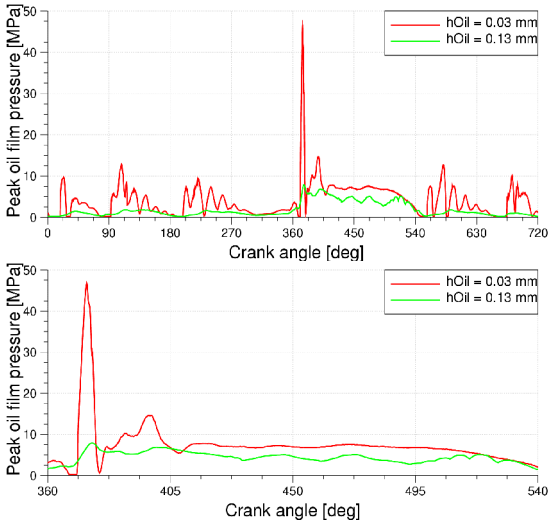

Figure 11: *Peak oil film pressure for one full cycle and zoomed for the expansion stroke*

In the next study, a constant oil film of 130μm, a nominal radial clearance of 10μm and an axialsymmetric piston skirt profile (Fig. 8a) were used in the calculation. In order to analyse the exact location of both small gap values between piston skirt and liner and the maximum oilfilm pressure values, a vertical scanning line was placed at the thrust-side of the piston skirt surface (Fig. 12).

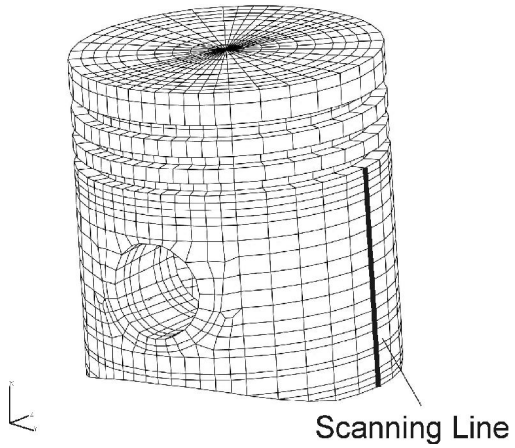

Figure 12: *Scanning line at thrust-side of piston skirt surface*

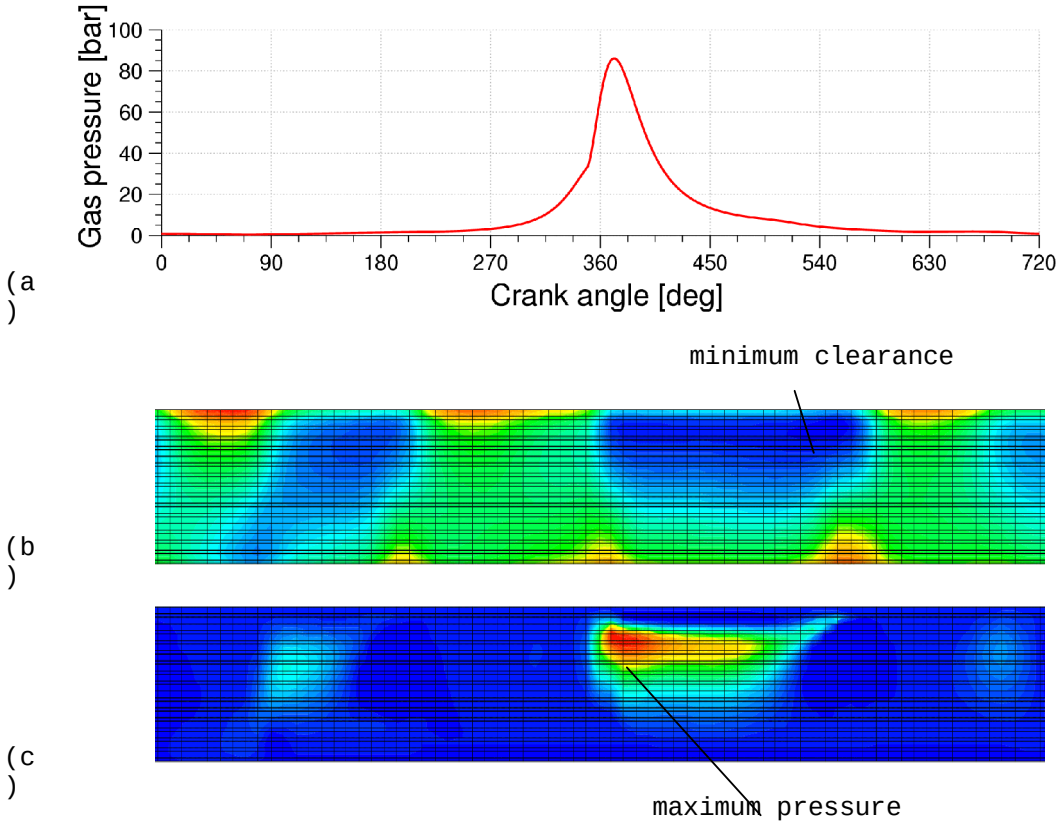

Figure 13: *Gas pressure upon piston top (a), clearance between piston skirt and liner (b) and the corresponding oilfilm pressure distribution (c) at scanning line*

In figure 13 the extracted results of clearance height (b) and pressure distribution (c) behaviour for one engine cycle (a) at the scanning line are shown. Via comparison of the clearance height animation over piston skirt height as well the tilting movement as the translatioal movement in direction of TS-ATS of the piston can be seen. Figure 13 (c) shows the corresponding pressure distribution. Due to the maximum gas pressure, especially after FTDC an area of small clearance height (17.5 μm) and maximum pressure (4.47 Mpa) can be located. Whereas pressure reduces significantly to a value of 2.69 Mpa the clearance value decreases slightly in the expansion stroke to a minimum value of 11.4 μm in the bottom dead center (540 deg.). This effect is caused by the additional tilting movement of the piston to the upper edge of the skirt in the last phase of the expansion stroke.

In order to be able to calculate the displacements, the velocities and the accelerations of degrees of freedom, that are not in the condensed set, (e.g. at outer cylinder wall surface), it is necessary to compute $\boldsymbol{q}$, $\dot{\boldsymbol{q}}$ and $\ddot{\boldsymbol{q}}$ of the uncondensed model too. This can be done easily, via the matrix multiplication given in equation 11.

This datarecovery was performed for the condensed results of the example discussed before. Figure 14 and 15 show the calculated distribution of integrated normal velocities of the uncondensed cylinder FE-model. The 0.5 kHz octave, the 1 kHz octave and the 2 kHz octave are shown in figure 14. The 1/3 octave band results analysed for 630 Hz, 1000 Hz and 2000 Hz are visualized in figure 15. Via comparison of the three results for both octave and 1/3 octave band, the maximum in 2 kHz octave band can be seen.

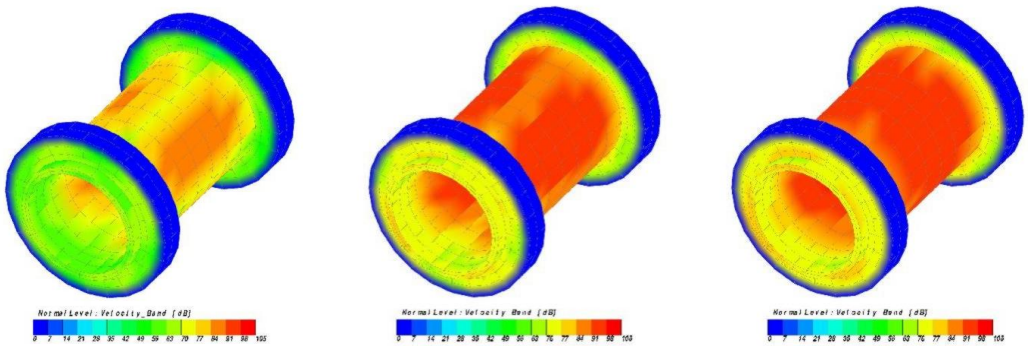

Figure 14: *Integrated velocities for 0.5 kHz octave, 1 kHz octave and 2 kHz octave*

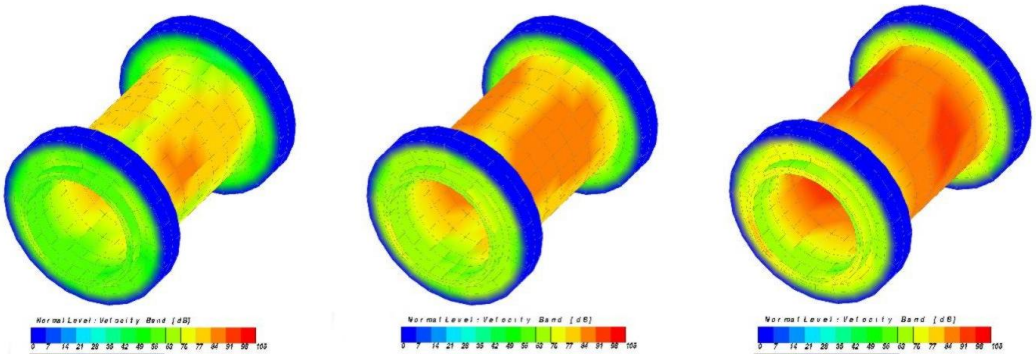

Figure 15: *Integrated velocities for 630 Hz 1/3 octave, 1 kHz 1/3 octave and 2 kHz 1/3 octave*

5. Summary and Outlook

Beside the theoretical background of the multibody simulation tool, the total simulation procedure (building up the model, perfoming the simulation, datarecovery to the uncondensed system) is presented in this pulication. The prediction procedure is now ready to be applied for contact improvement between piston and liner structure in order to reduce noise excitation, friction and wear.

The presented results are calculated using a one cylinder 4-stroke engine model. Future aspects in this ongoing project will be the simulation of vibrations of an entire engine in order to simulate absolute levels of structure borne noise and the evaluation of the calculated results on an engine test bed. These results will be described in future publications.

Acknowledgements:

The work described within this paper was funded by the Austrian Government and by the AVL List GmbH, Graz, Austria.

Nomenclature:

$f^{(a)}$ ..... External loads

f^{*} ..... Excitational loads

$\bar{f}$ ..... Condensed force vector

h , $\bar{h}$ ..... Clearance height

p , $\bar{p}$ ..... Oil film pressure

p^{*} ..... Inertia terms

q ..... Generalized displacement vector

q_a ..... Condensed displacement vector

t ..... Time

w ..... Axial velocity component

w_{Liner} ..... Axial velocity of liner

w_{Piston} ..... Axial velocity of piston

x ..... Circumferential direction

y , $\bar{y}$ ..... Gap direction

z , $\bar{z}$ ..... Axial direction

G_{ft} ..... Transfomation matrix

K ..... Stiffness matrix

$\bar{K}$ ..... Stiffness matrix of condensed system

D ..... Damping matrix

$\bar{D}$ ..... Damping matrix of condensed system

M ..... Mass matrix

$\bar{M}$ ..... Mass matrix of condensed system

η , $\bar{\eta}$ ..... Lubricant viscosity

θ , $\bar{\theta}$ ..... Fill ratio

Reference:

[1] Bathe, K.-J.: *Finite-Elemente-Methoden*, Springer Verlag, 1990

[2] DeLuca, J.C.: *The Influence of Cylinder Lubrication on Piston Slap*, Doctor-Thesis, Universidade Federal de Santa Catarina, Florianopolis, 1998

[3] *Excite Reference Manual (Version 5.0), AVL LIST GmbH,* Graz, 1999

PDF-XCHANGE Click to buy NOW! www.docu-track.com

[4] Kageyama, H.; Hara, S.; Kawabata, Y.: *Study of the Simulation of Piston Skirt Contact*, JSAE 9430095, Elsevier Science, 1994

[5] Kamp, H.; Spermann, J.: *New Methods of Evaluating and Improving Piston Related Noise in Internal Combustion Engines*, SAE Paper 951238, Detroit, 1995

[6] Krasser, J.: *Thermoelastohydrodynamische Analyse dynamisch belasteter Radialgleitlager*, Dissertation, Institut fuer Mathematik/C, TU Graz, 1996

[7] Knoll, G.; Peeken, H.; Lechtape-Grüter, R.; Lang, J.: *Computer Aided Simulation of Piston and Piston Ring Dynamics*, ASME ICE-Vol. 22, p 301, 1994

[8] Künzel, R.: *Die Kolbenbewegung in Motorquer- und Motorlängsrichtung, Teil 2: Einfluß der Kolbenbolzendesachsierung und der Kolbenform*, MTZ 56, S 534, 1995

[9] Priebsch, H. H.; Affenzeller, J.; Kuipers, G.: *Prediction Technique of Vibration and Noise in Engines*, Proceeding, IMechE Conference Quiet Resolutions, 1990

[10] Priebsch, H. H.; Krasser, J.: *Simulation of Vibration and Structure Borne Noise of Engines – A Combined Technique of FEM and Multi Body Dynamics* to be published at CAD-FEM USERS' MEETING, Bad Neuenahr – Ahrweiler, 1998